The age and depositional environments of the lower Karoo Moatize Coalfield of Mozambique: insights into the postglacial history of central Gondwana

Paulo Fernandes [a,*], Philip John Hancox [b], Márcia Mendes [c], Zélia Pereira [c], Gilda Lopes [a,d], João Marques [e], Raul Carlos Godinho Santos Jorge [f], Luís Albardeiro [c]

[a] *CIMA, Centre of Marine and Environmental Research\ARNET - Infrastructure Network in Aquatic Research, University of Algarve, Campus de Gambelas, 8000-139 Faro, Portugal*
[b] *Evolutionary Studies Institute, University of the Witwatersrand, PO Wits 2050, Johannesburg, South Africa*
[c] *Laboratório Nacional de Energia e Geologia (LNEG), Rua da Amieira, Apartado 1089, 4466-901, S. Mamede de Infesta, Portugal*
[d] *Plants, Photosynthesis and Soil Cluster, School of Biosciences, University of Sheffield, Alfred Denny Building, Western Bank, Sheffield S10 2TN, UK*
[e] *Gondwana Empreendimentos e Consultorias, Limitada, Rua 1.335, No. 233, Bairro da COOP, Maputo, Mozambique*
[f] *IDL - Instituto Dom Luiz, Departamento de Geologia da Faculdade de Ciências, Universidade de Lisboa, Campo Grande, Edifício C6, Piso 4, 1749-016 Lisboa, Portugal*

Abstract

The Moatize Coalfield belongs to a network of continental Karoo basins of central Mozambique, known as the Zambezi Basin. Palynological and sedimentological studies were performed on four coal exploration boreholes to determine the age, depositional settings, and overall geological evolution of its extensive coal deposits. Clastic formations recognised in this coalfield, in ascending order, are the Vúzi, Moatize and Matinde formations. Palynomorph assemblages indicate that the Moatize Coalfield succession ranges from Roadian (lower Guadalupian) to Changhsingian (upper Lopingian) in age. Two main depositional phases are identified, whose initiation and development are attributed to regional tectonic events and climate amelioration. The first phase formed towards the end of the deglacial period, characterised initially by fan deltas, represented by the upper Vúzi Formation, and the shift to lake–delta environments, represented by the lower part of the Moatize Formation. This phase took place from Roadian to the Wordian times. The lake–delta settings indicate a sediment aggradation trend with high subsidence rates in the lake basin, which, together with the associated post-glacial climate amelioration, led to the accumulation of coal deposits in swamps of the delta top and lake margins. The second depositional phase took place from Capitanian to Changhsingian times and related to fluvial environments initiated by uplift that reorganised the depocenter into alluvial plains characterised by bedload dominated rivers (braided) and overbank floodplains. Results obtained in this study provide critical information for the onset of the deglaciation events and the age of coal deposits in this part of Gondwana, important for wider stratigraphic correlation of these events in Africa and throughout the Gondwana.
© 2023 Elsevier B.V. and Nanjing Institute of Geology and Palaeontology, CAS. This is an open access article under the CC BY-NC-ND license (http://creativecommons.org/licenses/by-nc-nd/4.0/).

Keywords: Palynology; Guadalupian–Lopingian; coal seams; Karoo

---

* Corresponding author.
   E-mail address: pfernandes@ualg.pt (P. Fernandes).

1. Introduction

The accumulation of extensive coal deposits is one of the main features of the lower Karoo sedimentary sequences deposited in the Gondwanan basins of south-central Africa between the Late Palaeozoic Glaciation (LPG) and the end Permian mass extinction (Isbell et al., 2003, 2012; Fielding et al., 2008; Montañez and Poulsen, 2013; Montañez et al., 2016; Rosa and Isbell, 2021). The LPG termination and the subsequent onset of a greenhouse climatic trend in the depositional environments, and the time taken for the accumulation of the coal beds are, however, still a matter of discussion, particularly in the Karoo-aged basins of Mozambique (Isbell et al., 2012; Lopes et al., 2021a; Rosa and Isbell, 2021).

The Karoo Supergroup of the Main Karoo Basin (MKB) of South Africa is regarded as the most complete reference section, and forms the basis of correlation with all other African Karoo-aged basins. At the base of the Karoo Supergroup, the end of the LPG is diachronous between the southern (Shelf Facies) and northern (Valley Facies) margins of this basin (Visser, 1990). In the Shelf Facies, the last of the four deglaciation sequences documented, collectively forming the Dwyka Group, terminated at the end of the Sakmarian. In contrast, ice cover persisted in the Valley Facies until the Artinskian–Kungurian boundary (Visser, 1990; Millsteed, 1994). This age was recently confirmed by U-Pb zircon geochronology in ash layers at the basal beds of the post-glacial sequence (Griffis et al., 2019).

In the Karoo continental rift basins located to the north of the MKB (Catuneanu et al., 2005), including the Mozambique basins, the part of the stratigraphic sequence correlated to the Dwyka Group includes matrix-supported conglomerates, coarse-grained sandstones, laminated siltstones and mudstones, sitting unconformably upon Precambrian or Lower Palaeozoic basement rocks. These were deposited in glacial-terrestrial environments when glacier centres in the highlands expanded down into the rift valleys (Kreuser, 1987; Rosa and Isbell, 2021). Relying only on lithological similarities, these sequences have often been correlated to the Dwyka Group, and thus attributed to a Late Carboniferous–Early Permian (early Sakmarian) age (Paulino et al., 2010). The postglacial strata of these basins consist mainly of sandstones interbedded with mudstone and coals deposited in fluvial and lacustrine environments (Cairncross, 1989; Verniers et al., 1989; Oesterlen and Millsteed, 1994; Mugabe, 1999; Nyambe, 1999; Catuneanu et al., 2005; Kreuser and Woldu, 2010; Hancox, 2016; Bicca et al., 2017; Götz et al., 2020). The depositional age of the coal-bearing sequences in the Mozambican basins is still poorly constrained and has been correlated to the coal-bearing sequences of the Ecca Group at the northern margin of the MKB, which are of early Cisuralian (Asselian) to early Guadalupian age (Roadian) (GTK-Consortium, 2006; Modie and Le Hérissé, 2009; Paulino et al., 2010; Götz et al., 2020).

Recent studies on the Moatize-Minjova Sub-Basin coalfields in Mozambique highlighted problems with these stratigraphic correlations (Pereira et al., 2016, 2019; Lopes et al., 2021a). These studies have revealed noteworthy disparities from the existing knowledge about the region. The first is related to the occurrence (or not) of grounded subglacial tillites at the base of the Mozambican Karoo succession since such glacio-terrestrial sediments are commonly difficult to preserve due to erosion (Rosa and Isbell, 2021). Although, without disregarding the LPG, some of the first works on the Mozambican Karoo stratigraphy (Real, 1966) questioned the presence of lodgement till sediments at the base of the Karoo sequence, as angular clasts were scarce within the basal conglomerates, and no striae were observed in either the intraclasts or on the underlying Precambrian basement rocks (Real, 1966; Carvalho, 1977). The latter authors suggested that the basal conglomerates were the first post-glacial sediments deposited by fluvial processes. An alternative interpretation supports the presence of various fragmented ice centres over Gondwana, each waning at different times and at different rates (Isbell et al., 2021; López-Gamundí et al., 2021; Rosa and Isbell, 2021), as opposed to an extensive ice cap covering most of southern Gondwana (Crowley and Baum, 1992; Ziegler et al., 1997; Scotese, 2014).

The other problem was the age of the end of the LPG in Mozambique. Based on the palynological record, Lopes et al. (2021a) concluded that the basal post-glacial beds are no older than the Artinskian. Another important conclusion was that conglomerates younger than the mid-Cisuralian occur both at the base of the Karoo succession and interbedded in the sequence, thus denoting some tectonic control on the origin of some of the conglomeratic beds (Lopes et al., 2021b). These conclusions suggest that ice centers persisted until the Artinskian–Kungurian in the highlands that surrounded the Mozambican Karoo basins (Lopes et al., 2014; Pereira et al., 2014) and that tectonics had a significant role in the basin's development and depositional history (Bicca et al., 2017; Lopes et al., 2021b).

The age and depositional settings of the coal-bearing successions are also unresolved. Although recent studies from different Mozambican Karoo sub-basins provide valuable information on their depositional ages (Mahabeer, 2015, 2017; Pereira et al., 2016, 2019; Galasso et al., 2019; Götz et al., 2020; Lopes et al., 2021b), the stratigraphy of the various sub-basins is still not well-documented, making their correlation challenging (Lopes et al., 2021a). It becomes especially confusing where the stratigraphic correlation is based only on the succession of the coal seams and intra-seam sedimentary strata (Lakshminarayana, 2015), and not on the age of the stratigraphic sequences, thus masking the evolution of the different sedimentary environments in a tectonically active intracontinental basin.

To address the abovementioned problems, this work presents the relative ages of the Moatize Coalfield (MC) stratigraphic units, including the different coal seams

recognised, based on palynological cluster analysis. This analysis allowed the correlation of the entire coal-bearing stratigraphic succession of the MC. In addition, interpretations of the sedimentary environments based on lithological and sedimentological features, together with the palaeoecologically diagnostic palynomorphs, provide critical information for: the onset of the deglaciation events; the age of coal deposits; the sedimentary environment dynamics; the palaeoclimatic evolution; the formalisation of the stratigraphic units; and the overall geological evolution for this part of Gondwana, during Permian times.

2. Geological setting

The Mozambican coalfields outcrop extensively along the Zambezi Basin in the Tete Province. They comprise three sub-basins: i) the Moatize-Minjova Sub-Basin, ii) the Sanângoè-Mefidéze Sub-Basin, and iii) the Chicôa-Me cúcoè Sub-Basin (Afonso and Marques, 1993; Afonso et al., 1998; Hartzer et al., 2008) (Fig. 1). These are graben and half graben-type basins formed by tectonic reactivation, under extensional and transtensional stress, in Pan-African high-strain zones of the Zambezi Mobile Belt (Afonso, 1984; Orpen et al., 1989; Afonso et al., 1998; GTK-Consortium, 2006; Bicca et al., 2017). The current project focuses solely on the MC, the most intensively explored and exploited Karoo aged coalfield in Mozambique, where all the major active mines are located. The mining companies' core records also provide well-preserved stratigraphic sequences from this coalfield, including the Lower Karoo Supergroup type sections (Cairncross, 1989; Vasconcelos, 1995; GTK-Consortium, 2006; Vasconcelos and Achimo, 2010; Hancox, 2016).

The lower Karoo in the MC consists of three clastic units: the Vúzi, Moatize, and Matinde formations (GTK-Consortium, 2006; Fig. 2). The Vúzi Formation sits uncon-
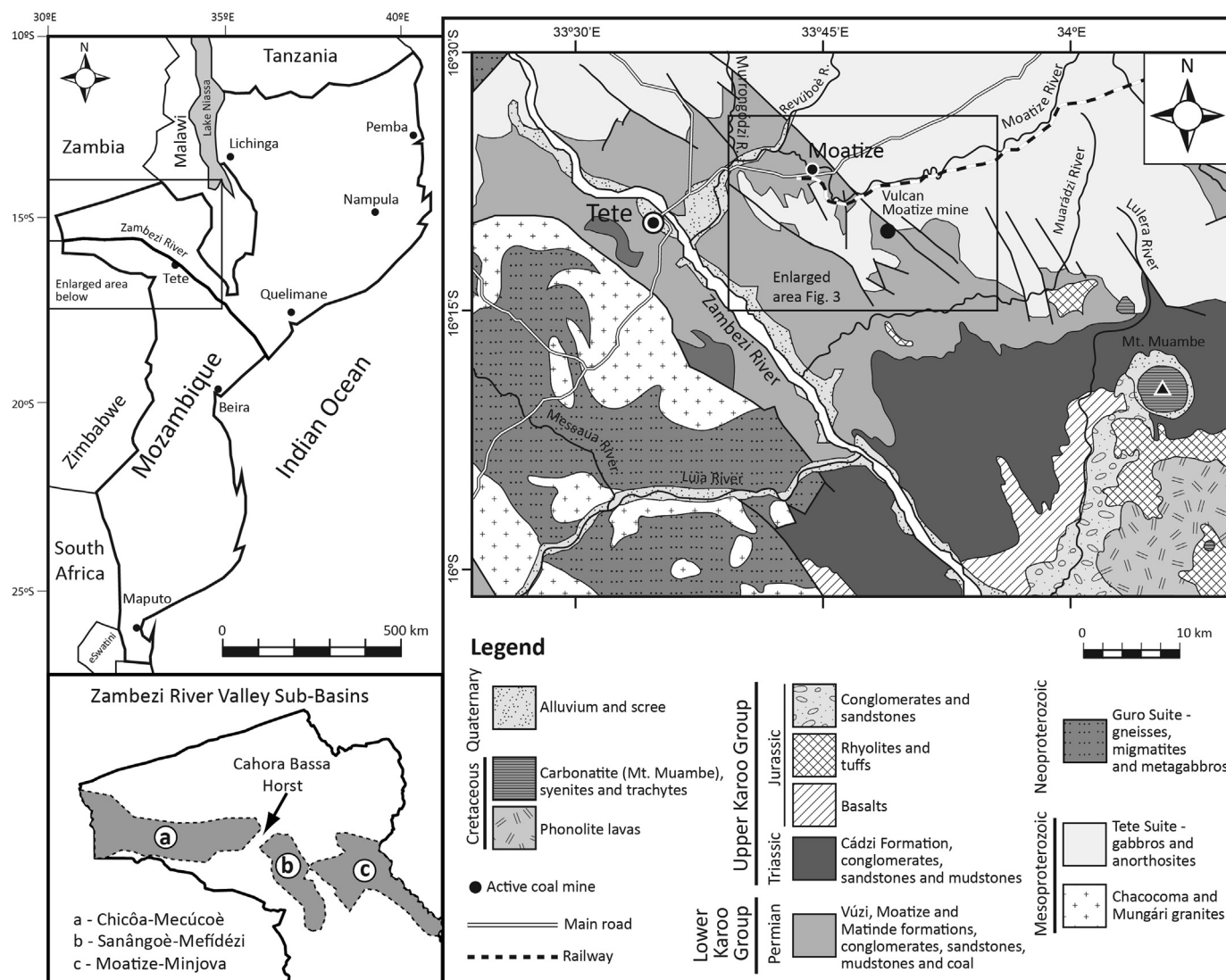

Fig. 1. Location of the study area in Tete Province in Mozambique and the Zambezi River Valley coal sub-basins. Simplified geological map adapted from the Geological Map of Mozambique at 1:1,000,000 scale (Hartzer et al., 2008).
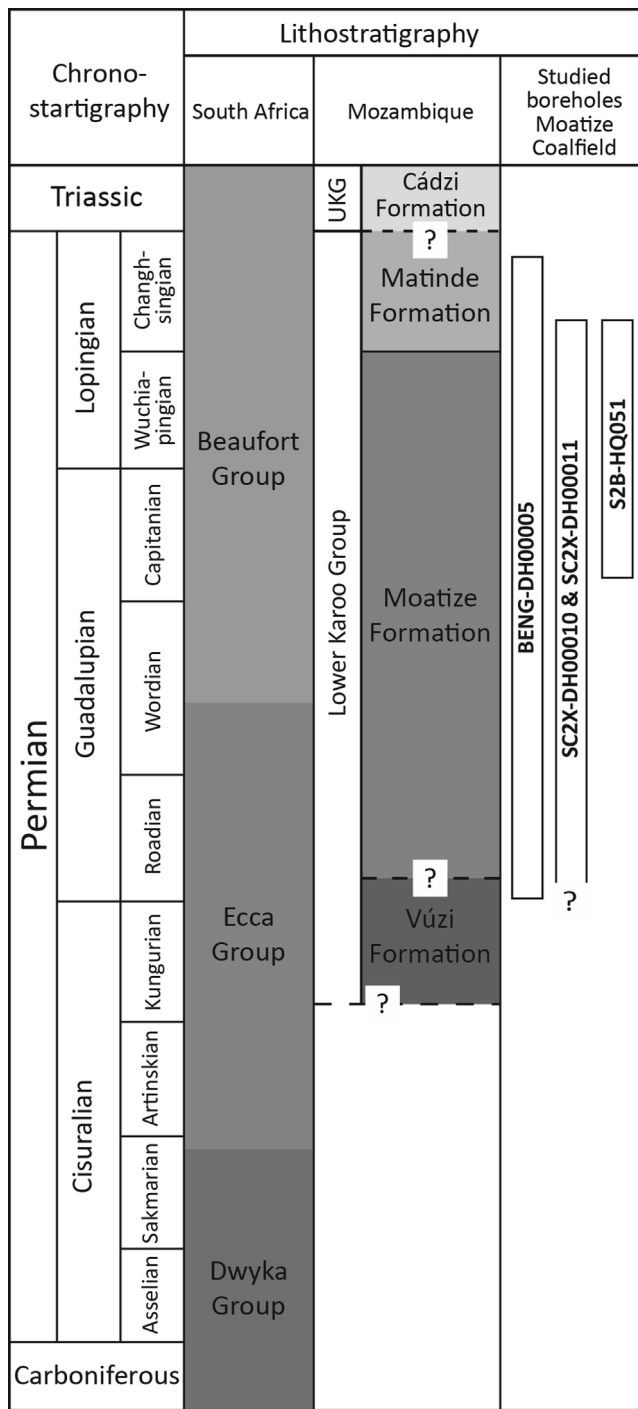
Fig. 2. Lithostratigraphic scheme for the Permian Moatize Coalfield (modified from Lopes et al., 2021a). UKG – Upper Karoo Group. The scheme is not to scale.

formably over Precambrian basement rocks and comprises interbedded matrix- to clast-supported conglomerates, sandstones, siltstones, mudstones, and occasionally coal seams. In the MC, the Vúzi Formation was described in the Murrongódzi River (Achimo et al., 2014; Pendkar et al., 2014) and has also been identified in numerous coal exploration boreholes (Lopes et al., 2014; Pereira et al.,

2014; Götz et al., 2020). In the Murrongódzi River section, the Vúzi Formation attains a thickness of ca. 100 m and was interpreted to be the result of fluvial to lacustrine processes in a periglacial setting (Achimo et al., 2014; Pendkar et al., 2014). A recent revision on the palynology of all Mozambican Karoo basins indicates that the Vúzi Formation is of Artinskian age (Lopes et al., 2021a).

The next unit, the Moatize Formation, conformably overlies the Vúzi Formation, and in the Moatize area it includes the workable coal seams (GTK-Consortium, 2006), replacing the term "Productive Series" used in the old literature (Real, 1966). The Moatize Formation consists of various carbonaceous-rich units of variable thicknesses intercalated with coarse- to fine-grained micaceous sandstones, siltstones, mudstones and rare conglomerates. The carbonaceous units include the workable coal seams and carbonaceous mudstones, siltstones, and fine-grained sandstones. Traditionally, the carbonaceous units have been named, from the oldest to youngest the Sousa Pinto (14 m thick), Chipanga (36 m thick), Bananeiras (27 m thick), Intermédia (22 m thick), Grande Falésia (12 m thick), and André (1 m thick) (Real, 1966). Only the Grande Falésia and André seams have not been regularly exploited. The depositional environments of the Moatize Formation varied from post-glacial lakes at the base to fluvial environments (braided) in the middle and upper part of the formation. The age of the Moatize Formation is still a matter of debate, but it most likely ranges from late Cisuralian to upper Guadalupian (Lopes et al., 2021a).

Culminating the Lower Karoo Group is the Matinde Formation, which conformably overlies the Moatize Formation. The Matinde Formation comprises coarse- to fine-grained sandstones, siltstones, mudstones, coal beds and conglomerates. The sandstone beds show sedimentary features (amalgamated beds, gravel lags at the base of sandstone beds, normal grading, planar and trough cross-stratification, and cross-lamination) that indicate fluvial channel fill deposits. The floodplain deposits of these fluvial systems are represented by siltstones, medium- to very fine-grained sandstones, mudstones and beds of coal. The Matinde Formation reaches a maximum thickness of ca. 2 km (GTK-Consortium, 2006). A middle Guadalupian to uppermost Lopingian age is most likely for the Matinde Formation (Pereira et al., 2016, 2019; Götz et al., 2017; Galasso et al., 2019; Lopes et al., 2021a).

3. Materials and methods

In this study, four coal exploration boreholes were analysed (Fig. 3). Boreholes SC2X-DH00010, SC2X-DH00011 and S2B-HQ051 are located near the boundary fault between the Mesoproterozoic Tete Suite and the MC. In contrast, borehole BENG-DH00005 is located ca. 4 km from an inlier of the Tete Suite, in an area of possible high subsidence rates in the MC (see discussion in 6.1.1). The stratigraphic succession in these four boreholes corresponds to the MC's typical Lower Karoo Group facies
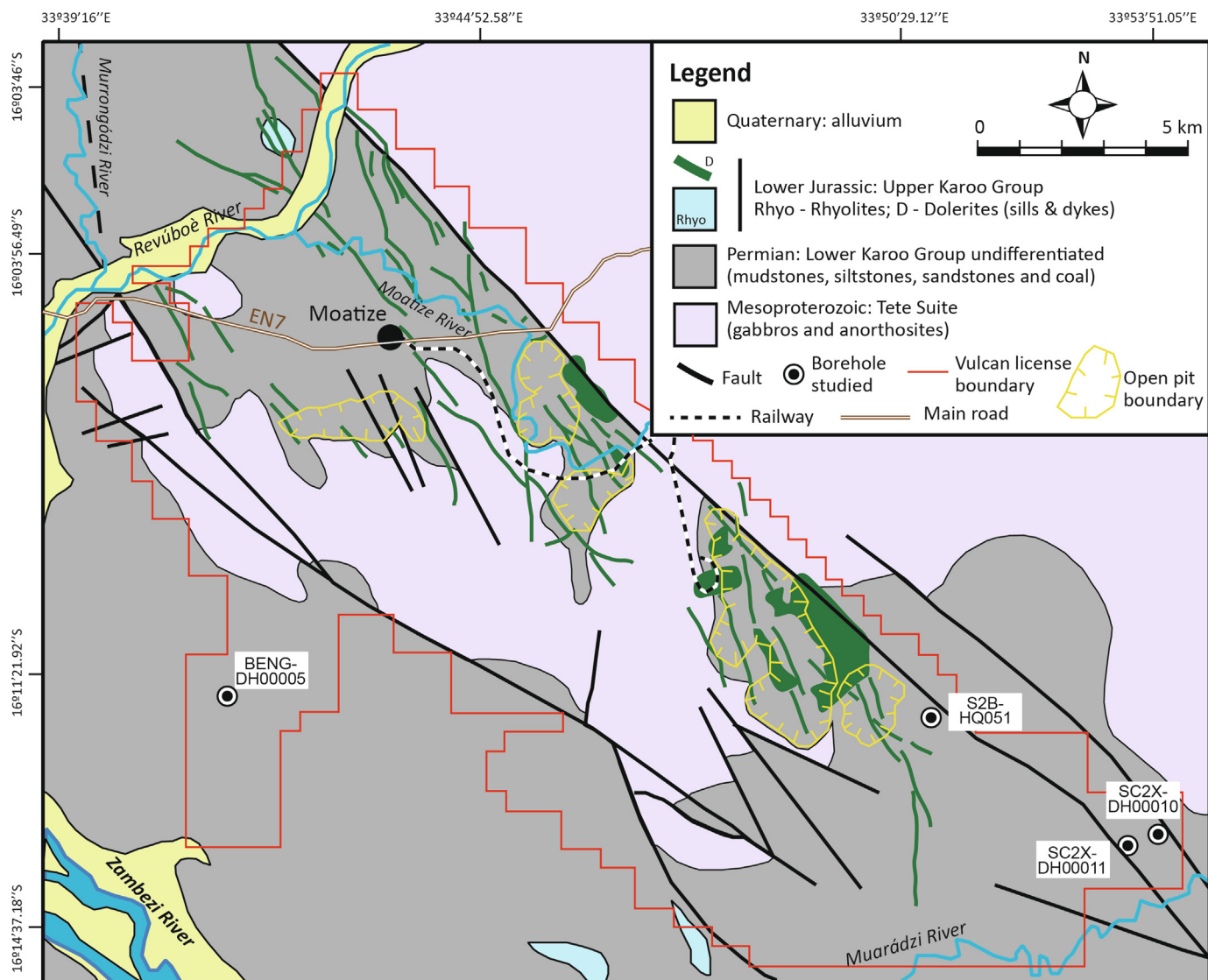
Fig. 3. Detailed geology of the Moatize Coalfield in the Tete region, with the location of the four boreholes. Adapted from the Geological Map of Mozambique, Sheet 1633, Tete, Geological Series 1:250,000, Direcção Nacional de Geologia, Maputo (GTK-Consortium, 2006).

(Vúzi, Moatize and Matinde formations) (Fig. S5). Since the dips from all the boreholes studied were minor (8° or less), they were not corrected; therefore, all depths provided throughout this work are based on downhole depths (Fig. S5).

The sedimentary succession in the four boreholes consists of clastic lithologies and coal beds of variable thickness. The stratigraphy of the boreholes can be organised according to the dominant sedimentary lithology at different depths in the cores of the boreholes, defining different lithofacies. Eight different lithofacies were considered: Cg1 (matrix-supported conglomerates), Cg2 (black carbonaceous matrix-supported conglomerates), S1 (very coarse-pebbly to medium-grained sandstones), S2 (very coarse to very fine-grained sandstones), S3 (medium- to fine-grained sandstones), SMh (heterolithic deposits), M (massive and fine laminated mudstones/siltstones), and C

(coal and carbonaceous mudstones), as described in Appendix A.

One hundred and ninety samples of mudstones and siltstones were collected for palynostratigraphy studies, distributed among the four boreholes: seventy-five samples from borehole BENG-DH00005, twenty-two samples from borehole S2B-HQ051, thirty-two samples from borehole SC2X-DH00011, and sixty-one samples from borehole SC2X-DH00010 (Figs. 3, S5). Detailed sampling levels were established below and above the main coal seams (Fig. S5). Tables S1–S4 refer to all the collected samples with an overview of the lithostratigraphic units, also shown in Fig. S6 with palynostratigraphic results obtained in this study.

All samples were processed at the National Laboratory of Energy and Geology (LNEG) using standard palynological laboratory procedures. Each rock sample weighing ca.

50 g followed the standard acid treatment, using HCl (37%) and HF (48%) acids to extract and concentrate the organic matter (Wood et al., 1996; Brown, 2008). The residues were oxidised using fuming nitric acid and were sieved using 20 μm mesh. The final residues were mounted on microscope slides using Entelan®, a commercial resin-based mounting medium. The slides were examined using Nikon Eclipse Ci and BX40 Olympus transmitted light microscopes.

The quantitative and qualitative distribution of the identified palynomorph assemblages is based on the relative abundance of the taxa and the first occurrences (FO) of specific key taxa. A minimum of 250 palynomorphs were counted for each slide, with the remainder being scanned for rare taxa. This number was not accomplished in some samples (Tables S1–S4), where the palynomorphs are extremely scarce, although the abundances have also been included. The quantitative analysis was discussed as follows: rare (< 5%), common (6–10%), frequent (11–20%), abundant (21–40%) and super-abundant (> 40%).

The biostratigraphic analysis was based on the palynostratigraphic schemes published by Galasso et al. (2019) and Pereira et al. (2019). The Tilia 1.7.16 software (Grimm, 1991) was used to display changes in the proportion of each sporomorph taxon, observe palynological trends over time, and plot the palaeoenvironmental analysis. Stratigraphically constrained sum-of-squares cluster analysis (CONISS; Grimm, 1987) was used to define local sporomorph assemblages and develop a palaeoenvironmental assessment of the MC. In these floral and palaeoenvironmental analyses, the palynomorphs were grouped into nine main categories adapted from Lindström and McLoughlin (2007): ferns, sphenophytes, lycophytes, glossopterids and non-glossopterids (Taeniate Bisaccate Pollen), non-taeniate bisaccate pollen, monosaccate pollen, asaccate pollen, and algae (Figs. S1–S4). The detailed graphics for the cluster analysis are presented as supplementary material (Figs. S1–S4). Likewise, Tables S1–S4 includes the sample details, lithostratigraphic units and results. Tables S5–S8 have all taxa identified in each sample and relative abundances (percentages). All samples, residues, and slides are held at the Palynological Collection of the LNEG in Portugal.

4. Palynostratigraphy

Eighty-eight palynomorph taxa were identified in this study (Figs. S1–S4). Sporomorphs are particularly susceptible to climate and environmental changes, in some cases presenting short stratigraphic ranges and becoming stratigraphically useful. Fig. S6 illustrates the CONISS cluster analysis's projected results for all boreholes, highlighting and correlating the coal seam sequences. By cluster analysis, barren or poorly preserved samples with low palynomorph counts were not placed into the well-defined clusters. Fig. S6 shows the cluster analysis concerning the lithostratigraphic data, complemented by the biostrati-

graphic key taxa interpretation. Selected taxa are presented and illustrated in Figs. 4, 5.

4.1. Early Guadalupian (Roadian) – Palynoassemblage A

Early Guadalupian (Roadian) age samples were associated with the top beds of the Vúzi Formation, and the basal beds of the Moatize Formation (sample BENG-DH00005-E05, sample SC2X-DH00010-A15). However, sporomorphs are very scarce in borehole SC2X-DH00010, and the rare occurrence of taeniate bissacate pollen grains such as *Protohaploxypinus* spp., *Striatopodocarpidites cancellatus* and *S. fusus* are documented in sample SC2X-DH00010-A15. The highly degraded and poorly preserved palynomorphs stand out. In sample BENG-DH00005-E05, the dominant occurrence of freshwater algae, such as chlorophycean, is highlighted.

4.2. Early–middle Guadalupian (probably late Roadian–Wordian) – Palynoassemblage B

Samples of early–middle Guadalupian (probably late Roadian–Wordian) age were associated with the Sousa Pinto coal seam (samples BENG-DH00005-E13–E17 and samples SC2X-DH00011-D10–D14) and Chipanga coal seam (samples BENG-DH00005-E18–E39). One of the distinctive characteristics of these assemblages is the dominance of freshwater algae. Biostratigraphically, the rare occurrence of *Cirratriradites africanensis* spores in borehole SC2X-DH00011 and the following pollen genus *Alisporites*, *Protohaploxypinus* (including *P. goraiensis*) and *Striatopodocarpites* (including *S. cancellatus*) characterise the assemblages.

4.3. Late Guadalupian (Capitanian) – Palynoassemblage C

The late Guadalupian (Capitanian) age samples were associated with the Bananeiras coal seam sequence (samples BENG-DH00005-E40–E47 and samples SC2X-DH00011-D15–D19). The base of this stage is defined by the FO of *Corisaccites alutas*, *Guttulapollenites hannonicus* and *Striatoabieites multistriatus*.

Significant heterogeneity between samples is highlighted, with some samples revealing notable pollen dominance (samples SC2X-DH00011-D15–D19). The trilete spore *Cirratriradites africanensis* continues to be documented, especially in samples from borehole SC2X-DH00011. Similarly, the bisaccate pollen grains dominate throughout the sequence, such as *Alisporites*, *Protohaploxypinus*, and *Striatopodocarpites*. Nevertheless, the non-taeniate bisaccate pollen *Allisporites* high percentage domain stands out, accompanied by a slight decrease to the top of the sequence of the taeniate bisaccate *Protohaploxypinus*. The rare to common occurrences of non-glossopterids are assigned to *Corisaccites alutas*, *Corisaccites* sp., *Guttulapollenites hannonicus*, and the pollen grains *Lueckisporites virkkiae*. Rare to common asaccate pollen
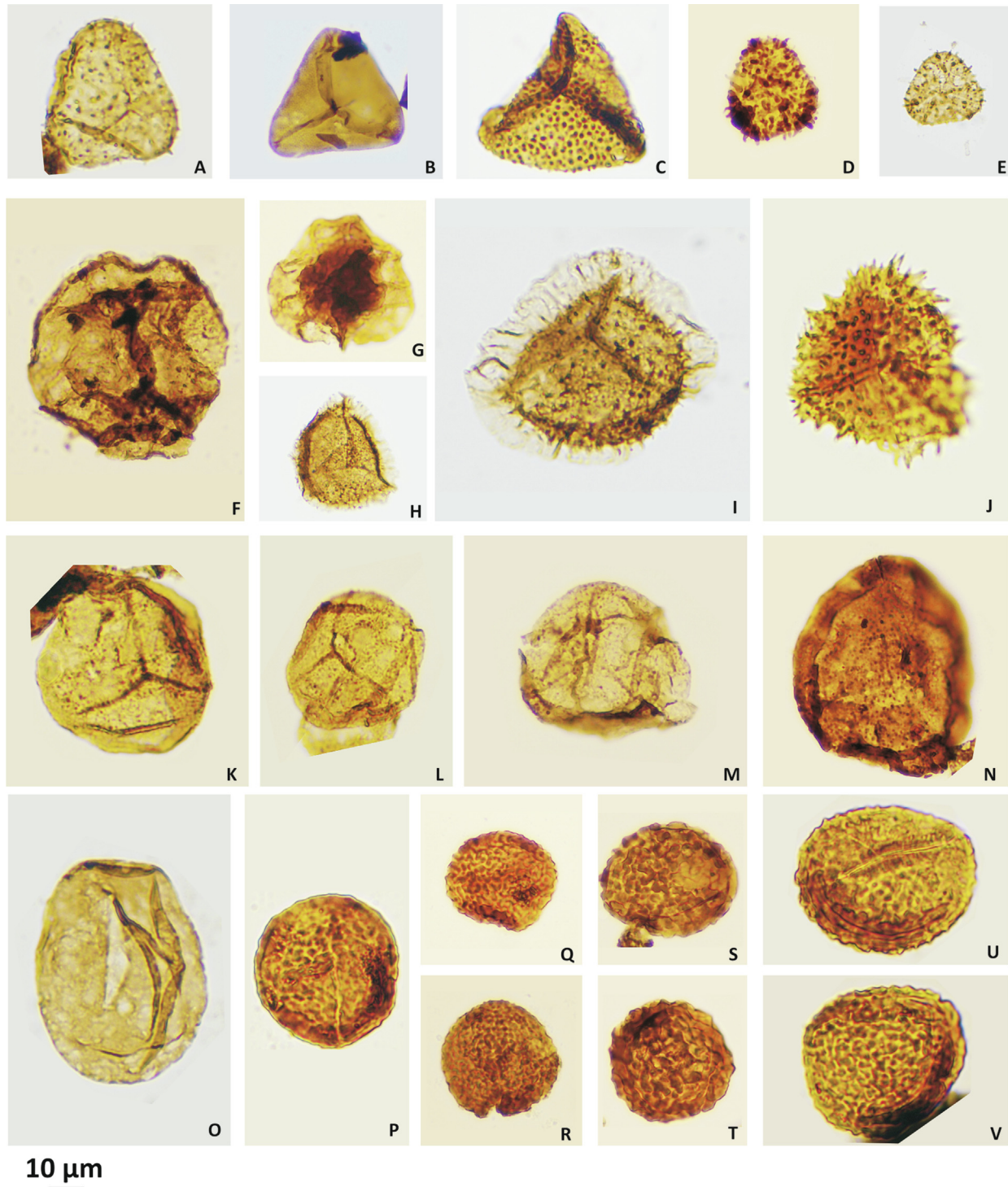
Fig. 4. Selected spore taxa. (A) *Apiculatisporis* sp., E69-1 sample, 1/24 slide, 1032/470. (B) *Microbaculispora trisina* (Balme and Hennelly) Anderson, E68-1 sample, 1/15 slide, 1023/460. (C) *Microbaculispora tentula* Tiwari, E69-1 sample, 1/81 slide, 1100/440. (D, E) *Horriditriletes tereteangulatus* (Balme and Hennelly) Backhouse; (D) C19-1 sample, 1/72 slide, 1086/442; (E) E69-1 sample, 1/101 slide, 1068/428. (F, G) *Aratrisporites* sp.; (F) E71-1 sample, 1/38 slide, 1090/422; (G) E71-1 sample, 1/50 slide, 1028/405. (H) *Cirratriradites* sp., E69-1 sample, 1/2 slide, 1008/476. (I) *Cirratriradites africanensis* Hart, E69-1 sample, 1/184 slide, 1091/335. (J) *Kraeuselisporites* sp., A52 sample, 1/72 slide, 924/328. (K–M) *Osmundacidites senectus* Balme; (K) A54 sample, 1/98 slide, 1092/377; (L) E74-1 sample, 1/62 slide, 1046/435; (M) C21-2 sample, 1/72 slide, 1078/408. (N) *Lundbladispora obsoleta* Balme, C18-1 sample, 1/57 slide, 1018/182. (O) *Laevigatosporites* sp., E69-1 sample, 1/57 slide, 1058/462. (P–R) *Thymospora pseudothiessenii* (Kosanke) Wilson and Venkatachala; (P) A53 sample, 1/47 slide, 1073/460; (Q) E73-1 sample, 1/76 slide, 1116/343; (R) E71-1 sample, 1/21 slide, 1047/456. (S–V) *Polypodiisporites* sp.; (S) E72-1 sample, 1/41 slide, 1115/458; (T) E74-1 sample, 1/58 slide, 1050/436; (U) A60 sample, 1/121 slide, 1070//420; (V) A53 sample, 1/72 slide, 1100/442.
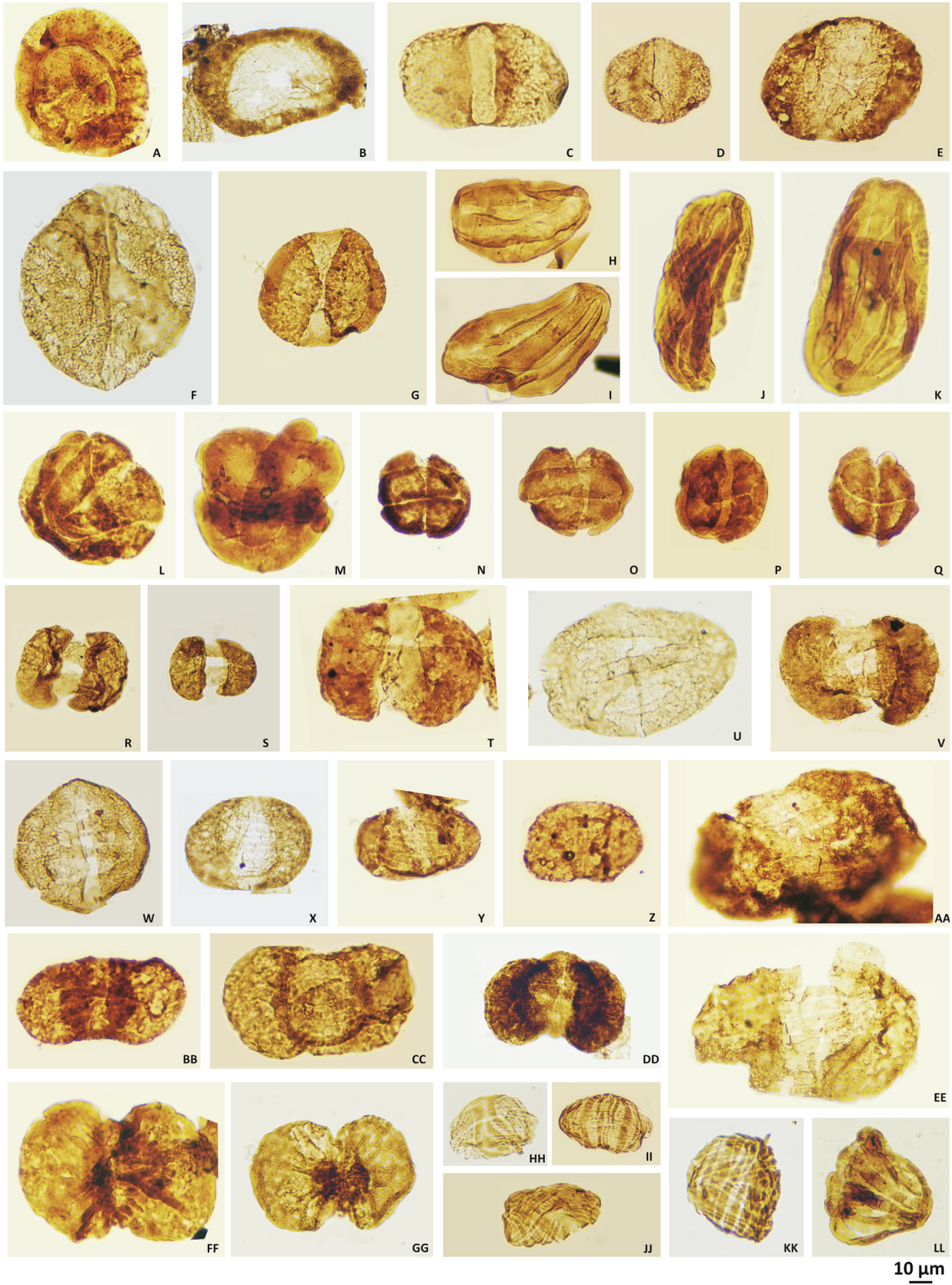
grains, such as *Vittatina* spp., *Pakhapites* spp., and *Weylandites lucifer*, also occur.

4.4. Early Lopingian (early Wuchiapingian) – Palynoassemblage D

Samples of early Lopingian (early Wuchiapingian) age were associated with the Intermédia coal seam sequence (sample BENG-DH00005-E48 and samples S2B-HQ051-C9–C14). The lowermost samples are characterised by abundant freshwater algae, with some samples revealing a significant dominance (sample S2B-HQ051-C14), and a low abundance of pollen grains, mainly represented by taeniate elements. The rare occurrences of non-glossopterids are assigned to *Guttulapollenites hannonicus*. The glossopterids pollen grains, such as *Alisporites*, *Protohaploxypinus* and *Striatopodocarpites*, are characteristic of the uppermost sample, where a decrease in freshwater algae also occurs. The sporadic, diagnosed occurrences of *Polypodiisporites* sp. and *Osmundacidites* sp., indicate a Lopingian age.

4.5. Middle Lopingian (middle to late Wuchiapingian) – Palynoassemblage E

Samples of middle Lopingian (middle to late Wuchiapingian) age were associated with the Intermédia coal seam sequence (samples BENG-DH00005-E49–E53 and samples SC2X-DH00010-A46–A48) and the Grande Falésia coal seam sequence (samples BENG-DH00005-E54–E57 and samples SC2X-DH00011-D20–D25). The common occurrence of *Thymospora pseudothiessenii* and *Polypodiisporites* sp. characterises the middle to late Wuchiapingian interval, as previously suggested in Galasso et al. (2019), Pereira et al. (2019), and Lopes et al. (2021b). The taeniate non-glossopterids *Lueckisporites* and *Corisaccites* pollen grains are documented throughout the sequence. The asaccate *Gnetaceaepollenites*, *Pakhapites* and *Vittatina* pollen grains are characteristic of

all samples in the stage except for the borehole BENG-DH00005. The glossopterids dominate the assemblage compared to the non-glossopterid pollen grains, with both having a general increasing trend to the top.

4.6. Late Lopingian (Changhsingian) – Palynoassemblage F

Samples of late Lopingian (Changhsingian) age are associated with the Grande Falésia coal seam (samples BENG-DH00005-E58–E61, samples S2B-HQ051-C16–C17, samples SC2X-DH00011-D26–D28, and samples SC2X-DH00010-A53–A55), unnamed coal seams, and André coal seam samples (samples BENG-DH00005-E64–E75, samples S2B-HQ051-C18–C22, and samples SC2X-DH00011-D29–D32). The FO of *Osmundacidites senectus* characterises the late Lopingian (Changhsingian) age, as indicated in previous MC studies (Galasso et al., 2019; Pereira et al., 2019; Lopes et al., 2021b). The top of the assemblage is not defined in this study.

Associated with the common occurrence of *Osmundacidites senectus*, characteristic of the Changhsingian age, species like *Protohaploxypinus microcorpus* and rare *Lunatisporites pellucidus* appear within the assemblage. This interval is also characterised by the fern spores increase assigned to *Thymospora* and *Polypodiisporites* forms. Although less frequently, the lycophytes *Cirratriradites* and *Kraeuselisporites* are commonly present throughout this assemblage. Scarce *Aratrisporites* sp. (samples BENG-DH00005-E70–E72) and *Lundbladispora* sp. (samples BENG-DH00005-E66–E74) are recognised in the uppermost samples.

The pollen record identified in the previous interval remains consistent. The rare asaccate *Gnetaceaepollenites*, *Pakhapites* and *Vittatina* pollen grains appear to be a constant at this palynoassemblage. Sporadic monosaccate pollen occurrences seem to be associated with the lowermost samples in the sequence (e.g., sample BENG-DH00005-E60). The glossopterids completely dominate the pollen assemblages, with non-glossopterids being residual.

Fig. 5. Selected key pollen taxa. (A) *Barakarites* sp., E72-1 sample, 1/5 slide, 1112/498. (B) *Cahenniasaccites ovatus* Bose and Kar, E69-1 sample, 2/4 slide, 952/403. (C) *Alisporites nilssoni* Balme, A48 sample, 1/188 slide, 1073/430. (D) *Alisporites gracilis* Segroves, C22-2 sample, 1/57 slide, 1037/170. (E) *Alisporites* sp., C19-2 sample, 1/14 slide, 1040/215. (F) *Alisporites potonie* (Lakhanpal, Sah and Dube) Somers, E69-1 sample, 1/72 slide, 956/447. (G) *Cedripites priscus* Balme, E71-1 sample, 1/61 slide, 1066/363. (H–K) *Gnetaceaepollenites sinuosus* (Balme and Hennelly) Bharadwaj; (H) E75-1 sample, 1/2 slide, 1023/503; (I) E75-1 sample, 1/101 slide, 1008/310; (J) A60 sample, 1/103 slide, 1063/457; (K) A60 sample, 1/268 slide, 1010/286. (L, M) *Guttulapollenites hannonicus* Balme; (L) A48 sample, 1/271 slide, 1010/332; (M) A57 sample, 1/76 slide, 993/473. (N, P) *Staurosaccites quadrifidus* (Dolby) Dolby and Balme; (N) C22-1 sample, 1/39 slide, 1050/478; (P) E74-1 sample, 1/19 slide, 1050/496. (O) *Corisaccites alutas* Venkatachala and Kar, E73-1 sample, 1/59 slide, 944/357. (Q) *Corisaccites* sp., E73-1 sample, 1/35 slide, 1010/505. (R, S) *Lueckisporites virkkiae* Potonie and Klaus; (R) A48 sample, 1/278 slide, 1041/384; (S) E69-1 sample, 1/153 slide, 1097/360. (T) cf. *Lunatisporites* sp., E73-1 sample, 1/83 slide, 1103/324. (U–W) *Lunatisporites* cf. *pellucidus* (Goubin) Helby; (U) E69-1 sample, 1/107 slide, 1081/427; (V) E71-1 sample, 1/107 slide, 985/164; (W) E69-1 sample, 1/267 slide, 987/175. (X) *Protohaploxypinus goraiensis* (Potonié and Lele) Hart, E69-1 sample, 2/26 slide, 1066/382. (Y, Z) *Protohaploxypinus limpidus* (Balme and Hennelly) Balme and Playford; (Y) C22-1 sample, 2/45 slide, 995/209; (Z) C20-1 sample, 1/11 slide, 977/433. (AA, EE) *Protohaploxypinus microcorpus* (Schaarchmidt) Clarke; (AA) C16-2 sample, 1/78 slide, 1092/274; (EE) C21-2 sample, 2/31 slide, 986/423. (BB, CC) *Protohaploxypinus* sp.; (BB) C18-1 sample, 1/65 slide, 975/172; (CC) A48 sample, 1/19 slide, 1062/327. (DD) *Striatopodocarpites cancellatus* (Balme and Hennelly) Hart, E69-1 sample, 1/235 slide, 1078/227. (FF, GG) *Striatopodocarpites fusus* (Balme and Hennelly) Potonié; (FF) A48 sample, 1/257 slide, 950/363; (GG) E69-1 sample, 1/96 slide, 985/434. (HH–JJ) *Weylandites lucifer* (Bharadwaj and Salujha) Foster; (HH) E69-1 sample, 1/61 slide, 968/452; (II) C16-2 sample, 1/91 slide, 966/258; (JJ) A57 sample, 1/104 slide, 985/458. (KK) *Weylandites magmus* (Base and Kar) Backhouse, E69-1 sample, 1/157 slide, 1003/357. (LL) *Vittatina* sp., A53 sample, 1/43 slide, 1063/454.

5. Lithofacies associations and sedimentary environmental interpretations

As shown in Fig. S5, two distinct lithofacies associations were recognised and named according to their interpreted depositional setting: Lake–Delta and Alluvial Plain. The latter association is further subdivided into Fluvial Channel-Belt and Overbank Floodplain sub-associations.

Although the stratigraphic profiles of the four boreholes correspond entirely to continental depositional settings, from lake–delta facies to alluvial plain facies, coal deposition is continuous throughout these environments. In the entire stratigraphic profiles, no sedimentary features nor processes of soil formation were observed, indicating prolonged subaerial exposure or arid conditions. This suggests that subaerial exposure of the different depositional settings of the basin, in particular the floodplain settings, occurred in poorly drained waterlogged conditions with high vertical aggradation rates.

6. Discussion

The palynological cluster analysis of the boreholes studied allowed for developing a temporal scheme for the stratigraphic sequence of the MC, vital for the lateral correlation of the stratigraphic successions, including the different coal seams across the coalfield. It also allowed a better understanding of the sedimentary environment changes from early Guadalupian to late Lopingian times. The identified two depositional phases are bounded by basin-wide tectonic processes that affect the architecture of the stratigraphy of different areas of the MC. Another critical factor for the basin evolution and the deposition of the coal seams was the long-term warmer climatic warming trend from Middle to Late Permian times, whose effects were superimposed on the depositional and tectonic processes that characterise this coalfield.

6.1. First depositional phase – Lake–Delta (Fig. 6A–C)

6.1.1. Depositional environments

The first depositional phase is recognised in boreholes BENG-DH00005, SC2X-DH00010 and SC2X-DH00011, encompassing the deposition of the Sousa Pinto and Chipanga coal seams (Fig. 6A, B). This deposition starts at the base by conglomerates and coarse-grained sandstones of the Vúzi Formation and ends with the Chipanga seam of the Moatize Formation. During this phase, deposition occurred from early to middle Guadalupian times.

The sedimentological analysis of this first cycle indicates the evolution from deglacial to lacustrine environments characterised by the accumulation of thicker layers of autochthonous coal at the end of the cycle in lake margin sedimentary environments. The Cg1 lithofacies that describe the Vúzi Formation suggest deposition in different depositional settings of fan deltas that ended in lakes produced by the retreat of mountain glaciers due to climate amelioration (Fig. 6A). Thus, they may correspond to sedimentation in outwash plains by bedload rivers, with subaerial and subaqueous mass-flows (Dietrich et al., 2019) formed by fault-controlled base-of-scarp coarse clastic deposition (Real, 1966; Carvalho, 1977), and in the glacial-lacustrine settings during peak ice melting phases (Achimo et al., 2014; Pendkar et al., 2014). We opt to place the boundary between the Vúzi and the overlying Moatize Formation at the top of the Cg1 and Cg2 lithofacies, following the explanation of the geological maps of Mozambique (GTK-Consortium, 2006). Thus, the thickness of the Vúzi Formation changes laterally, from ca. 30 to ca. 70 m in boreholes SC2X-DH00010 and SC2X-DH00011, respectively. Although in these boreholes, the Vúzi Formation could be thicker because their basal contact with the basement rocks was not intersected. Defining the Vúzi Formation in borehole BENG-DH00005 is more challenging because it lacks the lithofacies Cg1 at the base. Instead, the contact with the Precambrian basement rocks is made between carbonaceous mudstone and siltstones that pass upward to the first coal interval of the MC, which is tentatively attributed to the Vúzi Formation. The basal beds of this borehole are interpreted as lake floor and lake margin swamp settings corresponding to lateral facies of fan deltas. The presence of lithofacies Cg1 in the boreholes closer to the basin fault-boundary (SC2X-DH00010 and SC2X-DH00011) may suggest fault control on the deposition of this lithofacies. The diversity of depositional settings of the Vúzi Formation suggests that, since the initial phases of basin development, climate changes and regional tectonics played an essential role in the evolution of the sedimentary environments.

The deposition of the deglacial facies of the Vúzi Formation occurred mainly in the hanging walls of extensional faults having graben to half-graben geometries (Afonso, 1984; GTK-Consortium, 2006). We hypothesise that the rift shoulders persisted as mountainous regions with altitudes capable of withstanding ice centres until the early Guadalupian. These mountain regions delimited the MC to the north, south and probably to the east in today's coordinates. These mountainous ice centres progressively receded until they disappeared completely, most likely around late Roadian–Wordian times, marking the end of the Late Palaeozoic Ice Age (LPIA) in this region. This deglaciation phase provided large volumes of meltwater that drained to the lowland regions, forming sizeable lakes that started a new depositional phase (Kreuser and Woldu, 2010; Götz et al., 2020).

The formation of lakes and the network of fluvial braided channels that drained into them gave rise to the interdigitation of lacustrine and fluvial facies that characterise most of the stratigraphic sequence of this depositional phase. They formed a Lake–Delta sedimentary environment. A similar interpretation of the depositional environments of this part of the succession was described by Götz et al. (2020). During this stage, the lakes were probably confined to tectonic valleys flanked by
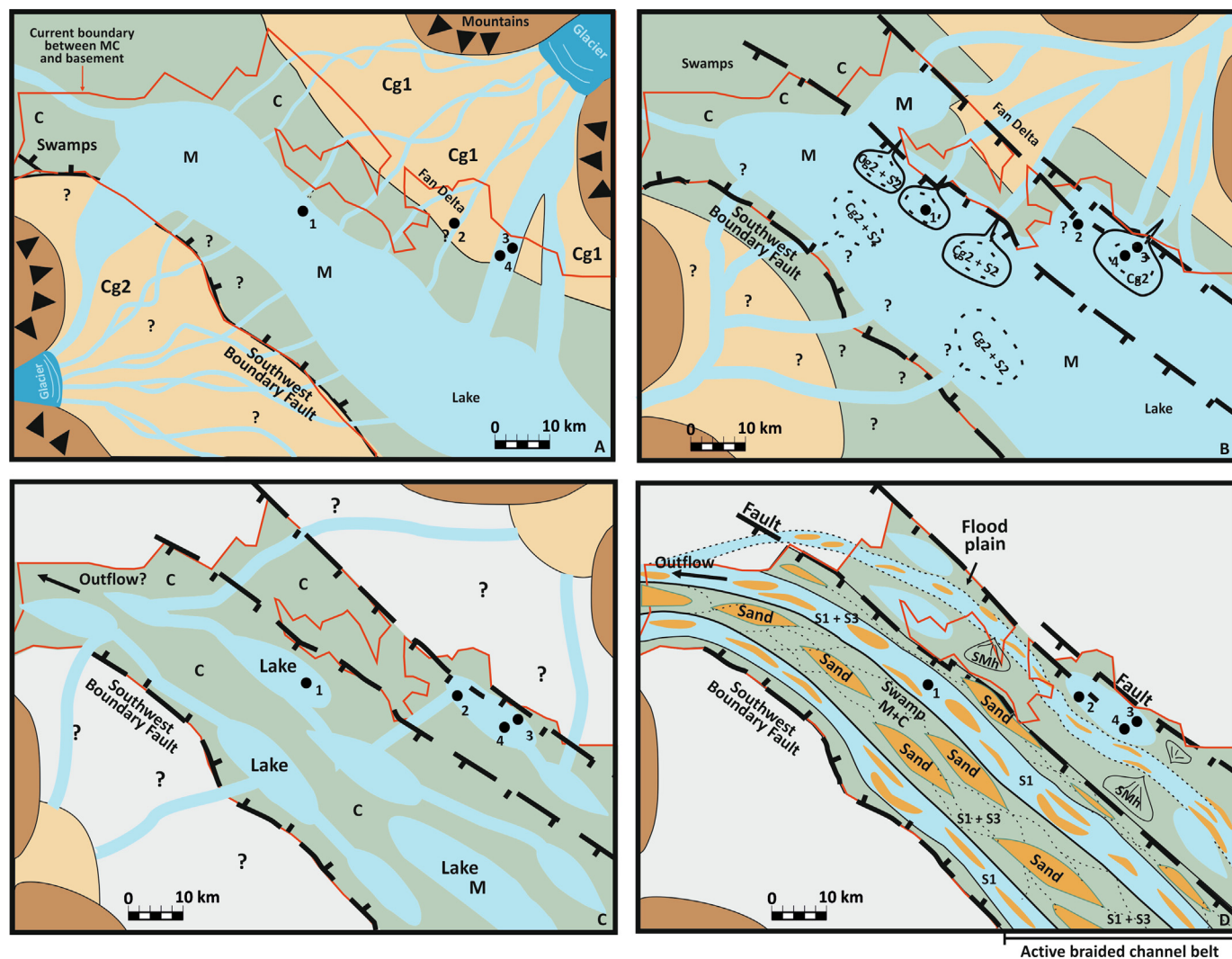
Fig. 6. Paleoenvironmental reconstructions. Note: The interpretations around the Southwest Boundary Block according to previous studies (Real, 1966; Mugabe, 1999; GTK-Consortium, 2006; Bicca et al., 2017). The numbers in the figure indicate the position of the boreholes: 1 – borehole BENG-DH00005, 2 – borehole S2B-HQ051, 3 – borehole SC2X-DH00010, and 4 – borehole SC2X-DH00011. (A) Fan Delta and lake phase – early Roadian (or older); initiation of the sedimentation in the basin. (B) Lake–delta, Roadian to Wordian – the maximum extension of the lakes characterised this time interval due to the fast melting of the glacier centres due to climate amelioration. (C) Chipanga seam – late Wordian to early Capitanian, characterised by a quiescence in the tectonic activity, which led to the infill of the lake depositional system. (D) Second Depositional Phase, Alluvial Plain – late Capitanian to late Lopingian, uplift of the entire region and a westward tilt of the Lake–Delta basin. See text for further explanation.

mountainous areas free of glacial ice, but whose higher elevations may have kept them humid. This was a phase of fluvial-lacustrine sediment aggradation in which the organisation of the lithofacies suggests that the slope at the entrance of the lakes was very gentle, allowing the existence of permanent and extensive wetlands and coal swamp regions on the lake margins, together with the existence of humid lake–deltas also characterised by extensive swamp environments. The accumulation of plant remains in these humid environments (lake margins and lake–delta plains) created the ideal conditions for accumulating the Sousa Pinto and Chipanga coal seams.

Clastic deposition occurred mainly by interdistributary rivers on the lake–delta plains (delta top) and the lake floor far from the lake margins by suspended sediment plumes (clays and silt). Transport by density currents may also have occurred on the lake floor and are attributed to lithofacies S2 recognised only in borehole BENG-DH00005. Plumes of water-laden sediments were transported by rivers to the lakes and were distributed around the lakes by surface currents induced by the wind. Eventually, they settled on the lake bottom, forming mud deposits rich in organic matter (M lithofacies), indicating prevailing anoxic conditions on the lake floor.

The interval of borehole BENG-DH00005 characterised by the intercalation of Cg2 and S2 lithofacies interpreted as subaqueous mass-flow deposits, could be attributed to a phase of intense extensional faulting localised near the position of this borehole. This borehole is located east and south of a small inlier comprising Mesoproterozoic

basement rocks (Fig. 3). A northwest-southeast trending normal fault has been proposed bounding the basement and the sedimentary rocks of the MC. The trend of this hypothesised fault is parallel to the main boundary faults of the MC, and it may have been an antithetic fault of the main western boundary fault, which limits the coalfield from the Mesoproterozoic metamorphic rocks of the Guro Suite. Thus, movements along this active fault may have caused gravity instability of sediments on the delta top and lake slope setting and triggered the mass flows. Some of these mass flows may have started as low-strength debris flows in which its turbulent parts scoured and mixed with the mud of the lake floor, forming the Cg2 lithofacies. However, this tectonic activity was restricted to where borehole BENG-DH00005 is located since no Cg2, and S2 lithofacies were recognised in the other borehole at the same stratigraphic position. This tectonic period occurred from late Roadian to Wordian time, and the partition created in the basin, may have been necessary for the following depositional cycle.

The deposition of the Chipanga coal seam, the thickest of the MC, marks the end of the Lake–Delta sedimentary phase, which may correspond to the uniformisation of the sedimentary environments characterised by extensive swamps and wetlands across the lake margins due to a prolonged phase of tectonic stability, which caused sediment aggradation to fill up the accommodation space available. This suggests that the lake system was most likely hydrologically closed during this first depositional phase, forming an endorheic drainage pattern. The lake level rose by meltwater from the waning LPIA ice centres. Uplifted crustal blocks formed by the initial tectonic basin formation processes, together with basement lithological heterogeneities amplified by glacial erosion during the LPIA, may have created the downstream barriers that confined the lake levels avoiding the lake from spilling over and becoming hydrologically open lake basins. Thus, the longitudinal profile of the drainage basins ended at these barriers (buttresses, according to Holbrook et al., 2006), and the base level of this Lake–Delta system was defined by the position of lake levels. In this context, the base level of the endorheic basins is controlled solely by the tectonics of the drainage basin and the climate conditions (Holbrook et al., 2006). Over time, if there are no significant variations between the rates of tectonic uplift and subsidence in the sedimentary basin, the base level rises, and the sedimentary pattern is one of sediment aggradation until the basin is filled (Nichols, 2004; Holbrook et al., 2006; Nichols and Fisher, 2007). The combination of the last processes may explain the extensive accumulation of the Chipanga seam.

The stratigraphic successions of the Lake–Delta depositional phase recognised in the boreholes are 150 to 250 m thick, indicating considerable sediment aggradation rates. The long-term preservation of these sedimentary sequences would have been possible due to the balance between 1) the rise of the buttress by tectonic processes, 2) the rise of the

lake levels due to the increase in river discharge during the deglaciation phases, and 3) the rates of subsidence in the sedimentary basin. The differential compaction of the coal and carbonaceous mudstones to clastic sediments cannot be discarded as a process that contributed to the increase in subsidence rates. The compaction ratio related to the coalification processes of peat to lignite and bituminous coals varies considerably from 2:1 to 11:1 (Ryer and Langer, 1980; Diessel, 1992; Shearer and Moore, 1996; Widera, 2015). Thus, if the conditions listed above were kept in balance in a steady state for a prolonged time, the early compaction of the extensive peat deposits would create more accommodation space for more organic-rich sediments to be deposited, allowing thick coal intervals to be formed. Using the methodology proposed by Large and Marshall (2015) for estimating the duration of coal seams, the calculated time for the deposition of the Chipanga seam is between 1.5 and 2.7 Ma, attesting to the prolonged time of quiescent climate and tectonic conditions during late Roadian–Wordian times.

Climatic conditions also strongly affect this depositional cycle, starting with cold, wet climates during the deglacial phase, followed by temperate humid climates during the lake sedimentary phase (Götz et al., 2020). With the climate amelioration, vegetation was fully established in the wetlands (lake margins and delta lakes) and upland regions (mountain ranges) of the drainage basin, promoting coal deposition in the wetlands and soil formation in upland areas. The development of forests in the uplands and the consequent increase in soil formation enabled landscape stabilisation and increased chemical weathering rates. This may profoundly impact the sediment yield of the fluvial systems by increasing the volume of sediments produced by chemical weathering (clays), reducing stream power and promoting deposition and aggradation of these fine-grained sediments in the fluvial-lacustrine settings.

There are differences, though, in the volume of clastic sediments and thicknesses of the lake sequences of the three boreholes where this sedimentary cycle was recognised. The lower part of the fluvial-lacustrine sequence in borehole BENG-DH00005 is sandstone rich, whereas mudstone, siltstones and coal dominate the same stratigraphic interval in boreholes SC2X-DH00010 and SC2X-DH00011. The lake facies thickness is also higher in borehole BENG-DH00005. These differences suggest differential subsidence rates between the borehole locations, with higher subsidence rates observed in borehole BENG-DH00005.

6.1.2. Palynological age

The palynological study of the coal seams sequences of the MC reflects the typical Permian *Glossopteris* province vegetation. The important biostratigraphic taxa are highlighted in this section. The flora and environment interpretation based on the palynomorph cluster analysis content is discussed for each coal seam succession. Coal deposition depends mainly on biomass production, climatic conditions, environmental stability, and development of the

contained clastic deposit, and ultimately is controlled by the basin tectonics (Retallack, 2013; Lopes et al., 2021b). All this data will be discussed below for the coals hosted in the Lake–Delta depositional phase.

The first interval of coal deposition corresponds to the stratigraphic interval that includes the top beds of the Vúzi Formation and basal beds of the Moatize Formation. The first palynological productive samples of the Moatize Formation yielded rare palynomorphs assigned to the Roadian age. The Roadian stage base is correlated to the FO of rare *Striatopodocarpidites cancellatus*, *S. fusus*, and *Protohaploxypinus* spp. (MacRae, 1988; Modie and Le Hérissé, 2009; Barbolini et al., 2016). The FO of *Striatopodocarpidites cancellatus* and *S. fusus*, together with the trilete spore *Cirratriradites africanensis*, indicates a Roadian age. The rare asaccate pollen grains *Gnetaceaepollenites sinuosus*, *Vittatina* spp., and *Weylandites lucifer* have also been observed in previous studies associated with the top beds of the Vúzi Formation and basal beds of the Moatize Formation (Lopes et al., 2014; Pereira et al., 2016, 2019). Therefore, a middle Roadian age is suggested for the base of the Moatize Formation.

The paleoclimate recorded during this stage was temperate and humid with well-established vegetation, characteristic of lowland areas related to lake margin coal swamps and lake–delta settings (predominance of higher seed ferns glossopterids, gymnosperms and rare lycopsids) with the rare influence of upland vegetation (monosaccate pollen grains are very scarce).

The following Sousa Pinto and Chipanga coal seams successions present an impoverished palynomorph assemblage, probably of late Roadian–Wordian age. Assemblages are marked by the occurrence of the spore *Cirratriradites africanensis* and rare pollen grains such as *Alisporites* spp., *Protohaploxypinus* spp. (including *P. goraiensis*) and *Striatopodocarpites* (including *S. cancellatus*).

The late Roadian–Wordian sequences are marked by a dominance of freshwater algae dominance (mainly chlorophycean algae single specimens and clusters). As confirmed in the lithofacies analysis, the monospecific algal bloom occurrences suggest lake depositional settings. These lakes may reflect the peak of the deglaciation period, providing a highly stratified water column with suitable accommodation space for the deposition of carbonaceous mudstones and lake margin coal seams. Therefore, lacustrine facies associations are assigned to the Sousa Pinto and Chipanga coal seams depositional sequences. The palynomorph assemblage, as documented, is relatively impoverished in variety. This diminished taxa diversity indicates that final deglaciation stages occurred in this part of the Gondwana during late Roadian–Wordian times.

6.2. Second depositional phase – Alluvial Plain (Fig. 6D)

6.2.1. Depositional environments

The second sedimentation cycle is dominated by fluvial processes, marking a clear contrast and change in sedimentary environments from the previous cycle. In detail, this depositional phase comprises smaller sedimentary cycles related to the river's dynamics and the position within the alluvial plain. The fluvial deposition occurred between the Capitanian (late Guadalupian) and the Changhsingian (late Lopingian). This depositional setting hosts the Bananeiras, Intermédia, Grande Falésia, André and other younger and unnamed coal seams, corresponding to the upper part of the Moatize Formation and lower part of the Matinde Formation.

The second depositional phase starts with coarse- to medium-grained sandstones, denoting a sudden increase in the energy of the sedimentary system. The sedimentary structures (erosive bases, metric thick sandstone beds showing normal grading, amalgamation, planar cross-stratification, planar cross-laminations) and their vertical organisation suggests deposition by bedload dominated river systems (probably braided), marking the beginning of the fluvial deposition within channel belt and overbank floodplains. In the braided channel belts, the volume of typical floodplain sediments (lithofacies SMh, M and C) is minimal compared to the channel-filling sandstones, denoting rapid aggradation of the channel belt, with capacity for lateral migration across the active alluvial plain.

The fluvial deposition phase is associated with an important basinwide tectonic event that tilted the basin floor by extensional faulting. This caused steeper gradients over the coal basin and its watershed. The steeper slopes caused fast flow, increasing the river's discharge and sediment transport as bedload. Therefore, an active braided channel belt occupied the previous lake basin. Measured palaeocurrents of sandstones beds (Mugabe, 1999; Bicca et al., 2017) indicated axial sediment supply (parallel to sub-parallel to the rift faults) with main currents flowing west-northwest and northwest (today's coordinates) and no sediment contribution from the rift flanks. The high thickness of the braided channel belt sandstones observed in borehole BENG-DH00005 suggests that this area was subject to higher subsidence rates than the areas where the other boreholes are located, close to the northeast fault margin of the basin (Fig. 3). These variations in subsidence rates could be attributed to the graben to half-graben basin geometry, as borehole BENG-DH00005 is located near one of the basin master faults, which corresponds to today's fault boundary near Tete city on the right bank of the Zambezi River. Close to this master fault is where the thickest Karoo succession of the MC is observed, with the preservation of the upper Karoo coarse clastics of the Cádzi Formation (GTK, Tete map), corroborating the high subsidence rates of this area. The northwest-southeast trending fault that separates borehole BENG-DH00005 from the other boreholes could be a minor antithetic normal fault of the last master fault, enhancing even further subsidence around the area of borehole BENG-DH00005, and controlling the lateral migration of the active channel belt. This fault control on the lateral migration of river channels could explain the observed contrast

in borehole BENG-DH00005 (dominated by channel-fill sandstones), regarding the lithofacies of the other boreholes, which are dominated by mudstones and coal that accumulated in floodplain settings.

Although we propose tectonism as the leading cause of the sedimentary shift from lake–delta to fluvial sedimentation, the contribution of climate change was also an important forcing factor for this shift. The palynological record presented here indicates that the fluvial deposition started during the Capitanian and extended to the early Lopingian. Biological crises and mass extinctions on the marine and terrestrial palaeoecosystems have been recognised during this time of Earth's history, caused by global climate changes. The main trigger for the end-Guadalupian mass extinction is still debatable; however, the effects of the Emeishan Large Igneous Province, which was active between 263 Ma and 259.1 ± 0.5 Ma (Zhou et al., 2002; Sun et al., 2010; Zhong et al., 2014) are considered the most likely cause since it occurred within the time duration of both marine and terrestrial mass extinctions (Day and Rubidge, 2021). Prolonged volcanic activity during the formation of Large Igneous Provinces (LIP) causes global temperature changes by releasing juvenile CO_2, causing warming, and SO_2 aerosols that cause cooling (Bond et al., 2014; Bond and Grasby, 2017), which consequently causes vegetation stress and demise. In terrestrial environments, the main effect of LIP volcanism is the increase of aridification by the sudden loss of vegetation cover caused by acid rain, overall toxicity, and the severe decrease in the photosynthetic activity of land plants due to the high concentration of aerosols in the atmosphere (Bond and Grasby, 2017). The record of the end-Guadalupian mass extinction inland in the Main Karoo Basin of South Africa has recently been evaluated (Day et al., 2015; Rey et al., 2018; Day and Rubidge, 2021). There is an apparent temporal association with the Emeishan LIP and an increase in the influx of coarse- to medium-grained clastic sediments to the basin at the extinction interval, suggesting increasing aridification (Bordy and Paiva, 2021). However, this is attributed to local tectonics of the Cape Fold Belt rather than to climatic changes that developed global arid climates (Rey et al., 2018; Day and Rubidge, 2021; Bordy and Paiva, 2021).

The increase in the influx of arenaceous sediments to the MC observed by the deposition of the braided channel belt can only tentatively be credited to increase aridification related to climate changes, since no other evidence of aridity (red beds, palaeosols and evaporites) was identified in this stratigraphic interval. Therefore, and without further evidence, regional tectonic events are believed to be responsible for the shift in the depositional environments from lake–delta to fluvial. Also, according to the palynological age, the base of the braided channel belt is of mid-Guadalupian and extended into late Lopingian without showing in the stratigraphy major changes in the depositional environments. Apart from the MKB of South Africa, regional tectonic events of end-Guadalupian age

were also documented in the Karoo basins of Tanzania (Wopfner and Jin, 2009) and Zambia (Yemane et al., 2002).

The coal seams intercalated with the thick sandstone packages in borehole BENG-DH00005 are interpreted as being formed in swamps created by the abandonment of braided channels due to lateral migration. The core profiles of boreholes SC2X-DH00010, SC2X-DH00011 and S2B-HQ051 that correspond to the fluvial depositional phase, as mentioned, are dominated overbank floodplain lithofacies, and the individual coal seams are more challenging to recognise because they rarely are separated by sandstone lithofacies. Therefore, some individual coal seams may be merged in the successions of the fluvial depositional phase of the last boreholes. Although some S1 and S3 lithofacies occur as isolated intervals separated by thick packages of floodplain deposits, indicating some fluvial dynamics over the locations of the last boreholes, these locations remained as more stable areas throughout the Lopingian.

The coal intervals of Lopingian age in boreholes SC2X-DH00010, SC2X-DH00011 and S2B-HQ051 are dominated by barcode coal, suggesting frequent flooding, where overbank coal swamps were repeatedly covered by the settling of mud, silt, and fine-grained sandstones, after flood peak, which was followed by the formation of new coal swamps. The presence of lithofacies SMh also attests to the prevalence of flooding events, interpreted as crevasse splay and thin flood sheets deposits, associated with lithofacies M in this part of the stratigraphic succession.

The upper ca. 110 m of the core in borehole BENG-DH00005 shows similar floodplain lithofacies as the fluvial successions of the other boreholes and can be tentatively attributed to the upper part of a thinning-upward fluvial cycle that starts with lithofacies S1, the base of which marks the boundary between the Moatize and Matinde formations. This situation may be related to a gradient reduction and discharge of the active braided channel belt, affecting its sediment transport capacity. This change seems more likely related to local tectonics or river dynamics than to a change in climate conditions, either global or regional. No clear sedimentological evidence corroborates different climate conditions affecting deposition for the four boreholes' Lopingian age intervals. However, the beginning of the deposition in braided channel belts can be tentatively correlated to a global climate event, as explained earlier, but this needs further investigation. Therefore, our hypothesised model for the deposition of the fluvial phase relates to the prolongation of regional tectonics events, whose major process during late Lopingian times was related to tectonic subsidence across the entire alluvial plain, but with more noticeable effects in the active channel belt (location of borehole BENG-DH00005) rather than the overbank floodplain settings (corresponding to the location of the other boreholes).

With time the river gradients were progressively reduced by fluvial aggradation; however, the accommodation space was not fully reduced because tectonic subsidence kept

pace with sediment supply to the basin and frequent flooding events caused floodplain aggradation. The 7 m thick bed of lithofacies Cg2 at 150 m depth in borehole S2B-HQ051 may be evidence of the continuation of the tectonic activity in the coalfield. This carbonaceous mud-supported conglomerate was deposited on a floodplain intercalated with coal. Its deposition could be related to tectonic activity where earthquakes-generating faulting created rupture topography that initiated localised mass flows over the floodplain settings in a process similar to that described by Jorgensen and Fielding (1999).

6.2.2. Palynological age

The development of the base of the Bananeiras coal seam sequence marks an evident change in vegetation, which is also associated with a major tectonic shift in the basin and the re-organisation of sedimentation from lake–delta to dominant fluvial sedimentation. The Bananeiras coal seam sequence is defined by the clear FO of the *Guttulapollenites hannonicus* key taxa and the FO of *Corisaccites alutas* and *Striatoabieites multistriatus* indicative of the earliest Capitanian (late Guadalupian) (palynoassemblage C). This early Capitanian data follows the correlations with the works of Götz et al. (2017, 2020) and Barbolini et al. (2018) for the Northern Karoo Basin. A Capitanian to early Lopingian age is proposed for the Bananeiras coal sequence.

Palynomorphs of samples younger than the Bananeiras coal seam yielded a moderately well-preserved, diverse assemblage, including numerous taxa and reflecting a luxuriant glossopterid vegetation dominated by bisaccate pollen grains *Protohaploxypinus* spp. and *Striatopodocarpites* spp. and gymnosperm pollen (*Alisporites* spp.). The first and rare occurrence of *Polypodiisporites* sp. and *Osmundacidites* sp., which become more common above this level, indicate a Lopingian age (palynossemblage D). The gymnosperm non-glossopterid pollen are rare to common and assigned to *Corisaccites alutas*, *Corisaccites* sp., *Guttulapollenites hannonicus*, and *Lueckisporites virkkiae*. The more substantial evidence for the presence of seed ferns evidence is assigned to the presence of rare to common *Vittatina* spp., *Pakhapites* spp., and *Weylandites lucifer*.

The FO of common to abundant *Thymospora pseudothiessenii* together with *Kraeuselisporites* spp., *Polypodiisporites mutabilis* and *Polypodiisporites* sp. (palynoassemblage E, equivalent to L2 Assemblage of Pereira et al., 2019), and the FO of *Osmundacidites senectus* together with the taxa described from the previous assemblages (palynoassemblage F, this study, corresponding to the L3 Assemblage of Pereira et al., 2019), defines the Intermédia and Grande Falésia coal seams.

Palynoassemblage E assemblage indicates the middle to late Wuchiapingian interval, while the palynoassemblage F depicts a late Lopingian (Changhsingian) age, as indicated in previous studies in the MC (Galasso et al., 2019; Pereira et al., 2019; Lopes et al., 2021b). Interestingly, the Intermédia and Grande Falésia coal seams are not always laterally

age correlative due to their position in the basin. The Intermédia coal seams sequence seems to be absent in borehole SC2X-DH00011.

The André coal seam and unnamed coal seams define the top sequence. The palynostratigraphic content is similar to the previous seam sequence, assigned to the palynoassemblage F of Changhsingian age, with common *Osmundacidites senectus* (Galasso et al., 2019; Pereira et al., 2019). This interval is also characterised by a fern spore increase assigned to *Thymospora* and *Polypodiisporites* forms. Near the top of the borehole profiles, the presence of the rare pollen taxa *Lunatisporites pellucidus* and *Protohaploxypinus microcorpus*, as well as lycophyte spores *Aratrisporites* sp. and *Lundbladispora* spp., allows for a correlation with the uppermost part of palynoassemblage F and indicates a latest Lopingian age (latest Permian; Galasso et al., 2019). Therefore, the André and the unnamed coal seams are assigned a Changhsingian age, reaching the latest Lopingian.

Palynological analysis indicates a flora of luxuriant vegetation where the higher seed ferns glossopterids completely dominate the pollen assemblages, with non-glossopterids being sub-dominant throughout the entire section, with both having a general increasing trend towards the top of the succession. Monosaccate pollen grains are scarce. Ferns and lycopsids are common to abundant and are the typical vegetation of humid and warm lowland areas, with the rare influence of upland vegetation (monosaccate pollen grains are scarce), related to vast swamps and shallow lakes environment existing during the deposition of the coal seam sequences.

7. Conclusions

The sedimentary infill of the MC denotes the interplay between regional tectonism and the climate amelioration trend that followed the end of the LPIA in southwestern Gondwana. Palynological cluster analysis allowed for the establishment of relative timelines, which is important for basin-wide correlation.

Early transtensional tectonism and the concomitant end of the LPIA created the initial accommodation space for the first depositional phase, which records the evolution from an initial deglacial fan delta to a lake–delta environment. The palynological age of the first depositional phase that hosted the Sousa Pinto and Chipanga seams is Roadian–Wordian (lower to mid-Guadalupian), and it encompasses the Vúzi and the lower part of the Moatize formations.

The beginning of the second depositional phase was linked to an important regional tectonic pulse that tilted the basin floor and uplifted the watershed. This led to a reorganisation of the sedimentary environments, with an alluvial system characterised by bedload dominated rivers and overbank floodplains. The boundary between the Moatize and Matinde formations would equate to renewing regional tectonic activity with uplift and the formation

of a new braided channel belt, as observed above the Grande Falésia Coal Seam. The fluvial depositional phase and the hosted coal seams range from the Capitanian to Lopingian ages and encompass the upper part of the Moatize Formation and the lower part of the Matinde Formation.

Besides the conclusions attained for the MC, our study made some important facts on the Karoo stratigraphy more evident, especially for the rift basins located north of the MKB. Our data support the diachronous terminus of the LPIA and the diachronous deposition of coals across the Karoo basins of southern Africa. In the case of the LPIA, a more likely scenario was the presence of several isolated ice covers on highlands that bordered these basins, which persisted until the early Guadalupian. Coeval glaciated and non-glaciated settings in the different basins may hamper the attempts to correlate the stratigraphy, sedimentary environments, and tectonism between these basins. The same arguments are applied to the coal deposits across the Karoo basins. In the MC, the coal deposition lasted from the early Guadalupian to the late Lopingian despite the prolonged active tectonic activity and climate amelioration.

In the rift basins located north of the MKB of South Africa, the classic vertebrate biostratigraphic (tetrapods) zonation cannot be applied due to the scarceness or absence of tetrapod fossils, as is the case of the MC, hampering the stratigraphic correlations. To overcome this difficulty, we used systematic palynostratigraphy based on cluster analysis and sedimentological analysis, which allowed us to obtain a more detailed geological evolution of the MC. The routine use of palynology can offer the tool to establish the essential biostratigraphic correlation schemes of the Permian for the Karoo basins in the same geological context as the MC, characterised by a strong tectonic control on the sedimentary processes.

Supplementary data

Supplementary data to this article can be found online at https://doi.org/10.1016/j.palwor.2023.07.001.

References

Achimo, M., Vasconcelos, L., Marques, J., Ferrara, M., 2014. Sedimentologia dos depósitos tilíticos do vale do Rio Murrongódzi, Bacia Carbonífera de Moatize-Minjova, Tete, Moçambique. 2° Congresso Nacional de Geologia e 12° Congresso de Geoquímica dos Países de Língua Portuguesa, Maputo, Moçambique, pp. 57–61.

Afonso, R.S., 1984. Ambiente geológico dos carvões gonduânicos de Moçambique - uma síntese. In: Lemos de Sousa, M.J. (Ed.), Symposium on Gondwana Coals, Lisbon, 1983. Proceedings and Papers. Comunicações dos Serviços Geológicos de Portugal 70, 205–214.

Afonso, R.S., Marques, J.M., 1993. Recursos Minerais da República de Moçambique. Contribuição para o seu conhecimento. 1st Edition. Instituto de Investigação Científica Tropical de Portugal e Direcção Nacional de Geologia de Moçambique, Lisboa, Portugal, 147 pp.

Afonso, R.S., Marques, J.M., Ferrara, M., 1998. Evolução Geológica de Moçambique. Instituto de Investigação Científica Tropical de Portugal and Direcção Nacional de Geologia de Moçambique, Lisboa, Portugal, 95 pp.

Barbolini, N., Smith, R.M.H., Tabor, N.J., Sidor, C.A., Angielczyk, K.D., 2016. Resolving the Madumabisa fossil vertebrates: Palynological evidence from the mid-Zambezi Basin of Zambia. Palaeogeography, Palaeoclimatology, Palaeoecology 457, 117–128.

Barbolini, N., Rubidge, B., Bamford, M.K., 2018. A new approach to biostratigraphy in the Karoo retroarc foreland system: Utilising restricted-range palynomorphs and their first appearance datums for correlation. Journal of African Earth Sciences 140, 114–133.

Bicca, M.M., Philipp, R.P., Jelinek, A.R., Ketzer, J.M.M., Scherer, C.M.D., Jamal, D.L., dos Reis, A.D., 2017. Permian–Early Triassic tectonics and stratigraphy of the Karoo Supergroup in northwestern Mozambique. Journal of African Earth Sciences 130, 8–27.

Bond, D.P.G., Grasby, S.E., 2017. On the causes of mass extinctions. Palaeogeography, Palaeoclimatology, Palaeoecology 478, 3–29.

Bond, D.P.G., Wignall, P.B., Keller, G., Kerr, A.C., 2014. Large igneous provinces and mass extinctions: An update. In: Keller, G., Kerr, A.C. (Eds.), Volcanism, Impacts, and Mass Extinctions: Causes and Effects. Geological Society of America, Special Papers 505, 29–55.

Bordy, E.M., Paiva, F., 2021. Stratigraphic architecture of the Karoo River channels at the end-Capitanian. Frontiers in Earth Science 8, doi: 10.3389/feart.2020.521766.

Brown, C.A., 2008. Palynological Techniques (2nd Edition). AASP Foundation, The Palynological Society, Dallas, Texas, 137 pp.

Cairncross, B., 1989. Paleodepositional environments and tectonosedimentary controls of the postglacial Permian coals, Karoo Basin, South Africa. International Journal of Coal Geology 12, 365–380.

Carvalho, L.H.B., 1977. Formações vulcânicas de Carinde, Tete-Moçambique. PhD thesis, Instituto Superior Técnico, Lisboa, Portugal, 213 pp.

Catuneanu, O., Wopfner, H., Eriksson, P.G., Cairncross, B., Rubidge, B.S., Smith, R.M.H., Hancox, P.J., 2005. The Karoo basins of south-central Africa. Journal of African Earth Sciences 43, 211–253.

Crowley, T.J., Baum, S.K., 1992. Modeling late Paleozoic glaciation. Geology 20, 507–510.

Day, M.O., Rubidge, B.S., 2021. The late Capitanian mass extinction of terrestrial vertebrates in the Karoo Basin of South Africa. Frontiers in Earth Science 9, doi https://doi.org/10.3389/feart.2021.631198.

Day, M.O., Ramezani, J., Bowring, S.A., Sadler, P.M., Erwin, D.H., Abdala, F., Rubidge, B.S., 2015. When and how did the terrestrial mid-Permian mass extinction occur? Evidence from the tetrapod record of the Karoo Basin, South Africa. Proceedings of the Royal Society B 282, 20150834.20150834.

Diessel, C.F.K., 1992. Coal-producing sedimentary environments. In: Diessel, C.F.K. (Ed.), Coal-Bearing Depositional Systems. Springer, Berlin, Heidelberg, pp. 349–459.

Dietrich, P., Franchi, F., Setlhabi, L., Prevec, R., Bamford, M., 2019. The nonglacial diamictite of Toutswemogala Hill (lower Karoo Supergroup, central Botswana): Implications on the extent of the late Paleozoic ice age in the Kalahari–Karoo Basin. Journal of Sedimentary Research 89, 875–889.

Fielding, C.R., Frank, T.D., Isbell, J.L., 2008. The late Paleozoic ice age — A review of current understanding and synthesis of global climate patterns. Geological Society of America, Special Papers 441, 343–354.

Galasso, F., Pereira, Z., Fernandes, P., Spina, A., Marques, J., 2019. First record of Permo-Triassic palynomorphs of the N'Condedzi sub-basin, Moatize-Minjova Coal Basin, Karoo Supergroup, Mozambique. Revue de Micropaléontologie 64, 100357.

Götz, A.E., Hancox, P.J., Lloyd, A., 2017. Permian climate change recorded in palynomorph assemblages of Mozambique (Moatize Basin, eastern Tete Province). Acta Palaeobotanica 57, 3–11.

Götz, A.E., Hancox, P.J., Lloyd, A., 2020. Southwestern Gondwana's Permian climate amelioration recorded in coal-bearing deposits of the Moatize sub-basin (Mozambique). Palaeoworld 29, 426–438.

Griffis, N.P., Montañez, I.P., Mundil, R., Richey, J., Isbell, J., Fedorchuk, N., Linol, B., Iannuzzi, R., Vesely, F., Mottin, T., da Rosa, E., Keller, B., Yin, Q.Z., 2019. Coupled stratigraphic and U-Pb zircon age constraints on the late Paleozoic icehouse-to-greenhouse turnover in south-central Gondwana. Geology 47, 1146–1150.

Grimm, E.C., 1987. CONISS: A FORTRAN 77 program for stratigraphically constrained cluster analysis by the method of incremental sum of squares. Computers & Geosciences 13 (1), 13–35.

Grimm, E.C., 1991. TILIA and TILIAGRAPH. PC Spreadsheet and Graphics Software for Pollen Data. In: INQUA Working Group on Data Handling Methods. Newsletter 4 (1990), 5–7.

GTK-Consortium, 2006. Map Explanation, Sheets 1630–1634, 1732–1734, 1832–1834 and 1932–1934. Geology of Degree Sheets Mecumbura, Chioco, Tete, Tambara, Guro, Chemba, Manica, Catandica, Gorongosa, Rotanda, Chimoio and Beira, Mozambique. Direcção Nacional de Geologia, Ministério dos Recursos Minerais, Maputo, Moçambique, 411 pp.

Hancox, P.J., 2016. The coalfields of south-central Africa: A current perspective. International Union of Geological Sciences 39, 407–428.

Hartzer, F.J., Manhiça, V.J., Marques, J.M., Grantham, G., Cune, G.R., Feitio, P., Daudi, E.X.F., 2008. Carta Geológica de Moçambique na escala 1:1000000. Direcção Nacional de Geologia, Ministério dos Recursos Minerais, Maputo, Moçambique.

Holbrook, J., Scott, R.W., Oboh-Ikuenobe, F.E., 2006. Base-level buffers and buttresses: A model for upstream versus downstream control on fluvial geometry and architecture within sequences. Journal of Sedimentary Research 76, 162–174.

Isbell, J.L., Lenaker, P.A., Askin, R.A., Miller, M.F., Babcock, L.E., 2003. Reevaluation of the timing and extent of late Paleozoic glaciation in Gondwana: Role of the Transantarctic Mountains. Geology 31, 977–980.

Isbell, J.L., Henry, L.C., Gulbranson, E.L., Limarino, C.O., Fraiser, M.L., Koch, Z.J., Ciccioli, P.L., Dineen, A.A., 2012. Glacial paradoxes during the late Paleozoic ice age: Evaluating the equilibrium line altitude as a control on glaciation. Gondwana Research 22, 1–19.

Isbell, J.L., Vesely, F.F., Rosa, E.L.M., Pauls, K.N., Fedorchuk, N.D., Ives, L.R.W., McNall, N.B., Litwin, S.A., Borucki, M.K., Malone, J.E., Kusick, A.R., 2021. Evaluation of physical and chemical proxies used to interpret past glaciations with a focus on the late Paleozoic Ice Age. Earth-Science Reviews 221, 103756.

Jorgensen, P.J., Fielding, C.R., 1999. Debris-flow deposits in an alluvial-plain succession: the Upper Triassic Callide Coal Measures of Queensland, Australia. Journal of Sedimentary Research 69, 1027–1040.

Kreuser, T., 1987. Late Paleozoic glacial sediments and transition to coal-bearing lower Permian in Tanzania. Facies 17, 149–157.

Kreuser, T., Woldu, G., 2010. Formation of euxinic lakes during the deglaciation phase in the Early Permian of East Africa. In: López-Gamundí, O.R., Buatois, L.A. (Eds.), Late Paleozoic Glacial Events and Postglacial Transgressions in Gondwana. Geological Society of America, Boulder, Colorado, pp. 101–112.

Lakshminarayana, G., 2015. Geology of Barcode type coking coal seams, Mecondezi sub-basin, Moatize Coalfield, Mozambique. International Journal of Coal Geology 146, 1–13.

Large, D.J., Marshall, C., 2015. Use of carbon accumulation rates to estimate the duration of coal seams and the influence of atmospheric dust deposition on coal composition. Geological Society, London, Special Publications 404, 303–315.

Lindström, S., McLoughlin, S., 2007. Synchronous palynofloristic extinction and recovery after the end-Permian event in the Prince Charles Mountains, Antarctica: implications for palynofloristic turnover across Gondwana. Review of Palaeobotany and Palynology 145, 89–122.

Lopes, G., Pereira, Z., Fernandes, P., Marques, J., 2014. Datação Palinológica dos Sedimentos Glaciogénicos da Formação (Tilítica) de Vúzi, sondagem ETA 65, Bacia Carbonífera de Moatize-Minjova, Moçambique - Resultados Preliminares. Actas do IX Congresso Nacional de Geologia. 2° Congresso de Geologia dos Países de Língua Portuguesa, Porto, Portugal, p. 100.

Lopes, G., Pereira, Z., Fernandes, P., Marques, J., Mendes, M., Gotz, A.E., 2021a. Permian stratigraphy and palynology of the Lower Karoo Group in Mozambique — a 2020 perspective. Newsletters on Stratigraphy 54, 335–362.

Lopes, G., Pereira, Z., Fernandes, P., Mendes, M., Marques, J., Jorge, R.C.G.S., 2021b. Late Permian palaeoenvironmental evolution of the Matinde Formation in the Muarádzi Sub-basin, Moatize-Minjova Basin, Mozambique. Journal of African Earth Sciences 176, 104138.

López-Gamundí, O., Limarino, C.O., Isbell, J.L., Pauls, K., Césari, S.N., Alonso-Muruaga, P.J., 2021. The late Paleozoic Ice Age along the southwestern margin of Gondwana: Facies models, age constraints, correlation and sequence stratigraphic framework. Journal of South American Earth Sciences 107, 103056.

MacRae, C.S., 1988. Palynostratigraphic correlation between the lower Karoo sequence of the Waterberg and Pafuri coal-bearing basins and the Hammanskraal plant macrofossil locality, Republic of South Africa. Memoirs of the Geological Survey of South Africa, 217 pp.

Mahabeer, K.C., 2015. Palynology of the Permian Ecca Mucanha-Vúzi Coal Basin, Tete Province, Mozambique. BSc thesis, University of Witwatersrand, Johannesburg, South Africa, 102 pp.

Mahabeer, K.C., 2017. Palynology of the Permian Sanângoè-Mefidezi Coal Basin, Tete Province, Mozambique and correlations with Gondwanan microfloral assemblages. MSc thesis, University of Witwatersrand, Johannesburg, South Africa, 168 pp.

Millsteed, B.D., 1994. Palynological evidence for the age of the Permian Karoo coal deposits near Vereeniging, northern Orange Free State, South Africa. South African Journal of Geology 97, 15–20.

Modie, B.N., Le Hérissé, A., 2009. Late Palaeozoic palynomorph assemblages from the Karoo Supergroup and their potential for biostratigraphic correlation, Kalahari Karoo Basin, Botswana. Bulletin of Geosciences 84, 337–358.

Montañez, I.P., Poulsen, C.J., 2013. The Late Paleozoic Ice Age: An evolving paradigm. Annual Review of Earth and Planetary Sciences 41, 629–656.

Montañez, I.P., McElwain, J.C., Poulsen, C.J., White, J.D., DiMichele, W.A., Wilson, J.P., Griggs, G., Hren, M.T., 2016. Climate, pCO_2 and terrestrial carbon cycle linkages during late Palaeozoic glacial–interglacial cycles. Nature Geosciences 9, 824–828.

Mugabe, J.A., 1999. Karoo deposits of Zambezi Graben – Moatize and Tete City Mozambique; Sedimentary facies distribution and palynological approach. PhD thesis, University of Utrecht, Utrecht, Netherlands, 297 pp.

Nichols, G., 2004. Sedimentation and base level controls in an endorheic basin: the Tertiary of the Ebro Basin, Spain. Boletin Geologico y Minero 115, 427–438.

Nichols, G.J., Fisher, J.A., 2007. Processes, facies and architecture of fluvial distributary system deposits. Sedimentary Geology 195, 75–90.

Nyambe, I.A., 1999. Tectonic and climatic controls on sedimentation during deposition of the Sinakumbe group and Karoo supergroup, in the mid-Zambezi Valley Basin, southern Zambia. Journal of African Earth Sciences 28, 443–463.

Oesterlen, P.M., Millsteed, B.D., 1994. Lithostratigraphy, palaeontology, and sedimentary environments of the western Cabora Bassa Basin, lower Zambezi Valley, Zimbabwe. South African Journal of Geology 97, 205–224.

Orpen, J.L., Swain, C.J., Nugent, C., Zhou, P.P., 1989. Wrench-fault and half-graben tectonics in the development of the Palaeozoic Zambezi Karoo Basins in Zimbabwe — the "Lower Zambezi" and "Mid-Zambezi" basins respectively — and regional implications. Journal of African Earth Sciences (and the Middle East) 8, 215–229.

Paulino, F., Vasconcelos, L., Marques, J., 2010. Estratigrafia do Karoo em Moçambique. Novas Unidades. 10° Congresso de Geoquímica dos Países de Língua Portuguesa e 16ª Semana da Geoquímica, Porto, Portugal, pp. 1285–1294.

Pendkar, N., Rubino, J.-L., Jean-Baptiste Baby, G., Sia, S.S.L., Prasetyotomo, W.S., 2014. Lower Karoo sedimentation in Moatize Basin, Mozambique: Analogue for understanding the deep rift sequence in offshore Rovuma Basin. Abstracts of the International Petroleum Technology Conference, Kuala Lumpur, Malaysia, pp. 1–11.

Pereira, Z., Lopes, G., Fernandes, P., Marques, J., 2014. Estudo palinoestratigráfico da sondagem ETA 72 do Karoo Inferior da Bacia de Moatize, Moçambique – Resultados Preliminares. Actas do IX Congresso Nacional de Geologia / 2° Congresso de Geologia dos Países de Língua Portuguesa, Porto, Portugal, p. 106.

Pereira, Z., Fernandes, P., Lopes, G., Marques, J., Vasconcelos, L., 2016. The Permian–Triassic transition in the Moatize-Minjova Basin, Karoo Supergroup, Mozambique: A palynological perspective. Review of Palaeobotany and Palynology 226, 1–19.

Pereira, Z., Fernandes, P., Lopes, G., Marques, J., Vaz, M., Costa, M., Correia, J., Castro, L., Galasso, F., 2019. Palynology of the Muarádzi sub-basin, Moatize-Minjova Coal Basin, Karoo Supergroup, Mozambique. Review of Palaeobotany and Palynology 269, 78–93.

Real, F., 1966. Geologia da Bacia do Rio Zambeze (Moçambique). Características geológico-mineiras da Bacia do rio Zambeze em território moçambicano. Junta de Investigações do Ultramar, Lisboa, Portugal, 183 pp.

Retallack, G.J., 2013. Permian and Triassic greenhouse crises. Gondwana Research 24, 90–103.

Rey, K., Day, M.O., Amiot, R., Goedert, J., Lécuyer, C., Sealy, J., Rubidge, B.S., 2018. Stable isotope record implicates aridification without warming during the late Capitanian mass extinction. Gondwana Research 59, 1–8.

Rosa, E.L.M., Isbell, J.L., 2021. Late Paleozoic Glaciation. In: Alderton, D., Elias, S.A. (Eds.), Encyclopedia of Geology (Second Edition). Academic Press, Oxford, pp. 534–545.

Ryer, T.A., Langer, A.W., 1980. Thickness change involved in the peat-to-coal transformation for a bituminous coal of Cretaceous age in central Utah. Journal of Sedimentary Research 50, 987–992.

Scotese, C.R., 2014. Atlas of Permo-Carboniferous paleogeographic maps (Mollweide projection), maps 53–64, The Late Paleozoic. PALEOMAP Atlas for ArcGIS, PALEOMAP Project, Evanston, IL.

Shearer, J.C., Moore, T.A., 1996. Effects of experimental coalification on texture, composition and compaction in Indonesian peat and wood. Organic Geochemistry 24, 127–140.

Sun, Y., Lai, X., Wignall, P.B., Widdowson, M., Ali, J.R., Jiang, H., Wang, W., Yan, C., Bond, D.P.G., Védrine, S., 2010. Dating the onset and nature of the Middle Permian Emeishan large igneous province eruptions in SW China using conodont biostratigraphy and its bearing on mantle plume uplift models. Lithos 119, 20–33.

Vasconcelos, L., 1995. Contribuição para o conhecimento dos carvões da Bacia Carbonífera de Moatize, Província de Tete, República de Moçambique. PhD thesis, Universidade do Porto, Porto, Portugal, 231 pp.

Vasconcelos, L., Achimo, M., 2010. O carvão em Moçambique. In: Cotelo Neiva, J.M., Ribeiro, A., Mendes Victor, L., Noronha, F., Ramalho, M.M. (Eds.), Ciências Geológicas – Ensino e Investigação da sua História. Geologia das Ex-Colónias de África, Lisboa, Portugal, pp. 191–206.

Verniers, J., Jourdan, P.P., Paulis, R.V., Frasca-Spada, L., De Bock, F.R., 1989. The Karoo Graben of Metangula Northern Mozambique. Journal of African Earth Sciences (and the Middle East) 9, 137–158.

Visser, J.N.J., 1990. The age of the late Palaeozoic glacigene deposits in Southern Africa. South African Journal of Geology 93, 366–375.

Widera, M., 2015. Compaction of lignite: A review of methods and results. Acta Geologica Polonica 65, 367–368.

Wood, G.D., Gabriel, A.M., Lawson, J.C., 1996. Palynological techniques-processing and microscopy. In: Jansonius, J., Mcgregor, D.C. (Eds.), Palynology: Principles and Applications, Vol. 1. American Association of Stratigraphic Palynologists Foundation, Salt Lake City, Utah, pp. 29–50.

Wopfner, H., Jin, X.C., 2009. Pangea megasequences of Tethyan Gondwana-margin reflect global changes of climate and tectonism in Late Palaeozoic and Early Triassic times — A review. Palaeoworld 18, 169–192.

Yemane, K., Grujic, D., Nyambe, I., Renaut, R.W., Ashley, G.M., 2002. Paleohydrological signatures and rift tectonics in the interior of Gondwana documented from Upper Permian lake deposits, the Mid-Zambezi Rift Basin, Zambia. In: Renaut, R.W., Ashley, G.L. (Eds.), Sedimentation in Continental Rifts. SEPM Society for Sedimentary Geology, Tulsa, Oklahoma, pp. 143–162.

Zhong, Y.T., He, B., Mundil, R., Xu, Y.G., 2014. CA-TIMS zircon U–Pb dating of felsic ignimbrite from the Binchuan section: Implications for the termination age of Emeishan large igneous province. Lithos 204, 14–19.

Zhou, M.F., Malpas, J., Song, X.Y., Robinson, P.T., Sun, M., Kennedy, A.K., Lesher, C.M., Keays, R.R., 2002. A temporal link between the Emeishan large igneous province (SW China) and the end-Guadalupian mass extinction. Earth and Planetary Science Letters 196, 113–122.

Ziegler, A.M.H., Hulver, M.L., Rowley, D.B., 1997. Permian World topography and climate. In: Martini, I.P. (Ed.), Late Glacial and Postglacial Environmental Changes: Quaternary Carboniferous–Permian, and Proterozoic. Oxford University Press, Oxford, pp. 111–146.